의학석사 학위논문

Gel phantom study with HIFU: Influence of metallic stent containing either air or fluid

고강도 집중 초음파의 겔 모형 연구:

공기 또는 유체를 포함한 금속 스텐트의 영향

2014년 02월

서울대학교 대학원

의학과 영상의학 전공

강 경 미

의학석사 학위논문

고강도 집중 초음파의 겔 모형 연구:
공기 또는 유체를 포함한 금속 스텐트의 영향

Gel phantom study with HIFU:
Influence of metallic stent
containing either air or fluid

February 2014

The Department of Radiology,

Seoul National University

College of Medicine

Koung Mi Kang

고강도 집중 초음파의 겔 모형 연구:
공기 또는 유체를 포함한 금속 스텐트의 영향

지도교수 이 재 영

이 논문을 의학석사 학위논문으로 제출함

2014 년 2 월

서울대학교 대학원

의학과 영상의학 전공

강 경 미

강경미의 의학석사 학위논문을 인준함

2013 년 12 월

위 원 장 김 용 태 (인)

부위원장 이 재 영 (인)

위 원 조 정 연 (인)

ABSTRACT

Purpose: We aimed to investigate whether a cylindrical structure containing either air or fluid and with or without a metallic stent affects the volume and density of cavitation produced by high-intensity focused ultrasound (HIFU) via a gel phantom study.

Materials and Methods: Sixteen phantoms with a cylindrical hole were divided into 4 groups of 4 phantoms with air in the holes (Group 1), 4 phantoms with fluid in the holes (Group 2), 4 phantoms with air-containing metallic stents (Group 3), and 4 phantoms with fluid-containing metallic stents (Group 4). The VIFU-2000 small animal HIFU unit (ALPINION Medical Systems, Seoul, Korea) was used with acoustic power (100W), exposure time (36 sec.), duty cycle (50%) and pulse repetition frequency (40 Hz). The focus of the HIFU beam was placed at the posterior wall of the hole in the phantom. The size of cavitation on x-, y-, and z-axis was measured, and the volume of cavitation and coagulation was calculated using the formula for the volume of an elliptical cone. The density of cavitation was measured in the tissue phantom anterior to the hole with 1cm x1cm square region of interest. For statistical analysis, Kruskal-Wallis test and Mann-Whitney U test were used.

Results: The volume of anterior cavitations of Groups 1 and 3 were significantly larger than those of Groups 2 and 4 ($P < .05$). The volume of posterior cavitations of Groups 1, 2, 3 and 4 were not significantly different each other ($P > .05$). The size on all axes and volumes of anterior cavitations

were significantly larger than those of posterior cavitations only in Groups 1 and 3 (all $P < .05$). Regarding the density, anterior cavitations of Groups 1 and 3 were significantly denser than that of Groups 2 and 4. ($P < .05$).

Conclusion: Phantoms with air-containing holes developed larger and denser cavitations anterior to the focus without unnecessary coagulation posterior to the focus, regardless of the presence of stents. The result of this study might be applied to maximize cavitation to enhance drug delivery into tumors before air-containing duct or stent.

Keywords: High-intensity focused ultrasound (HIFU), Cavitation, Pancreatic neoplasms, Stent, Air, Fluid, Phantom study

Student number: 2012-21670

CONTENTS

LIST OF TABLES AND FIGURES

LIST OF ABBREVIATIONS

HIFU = high-intensity focused ultrasound

CBD = common bile duct

BSA = bovine serum albumin

INTRODUCTION

Unresectable pancreatic cancer is a topic of current interest in the clinical application of high-intensity focused ultrasound (HIFU). Because approximately 80% of patients have unresectable disease at the time of diagnosis and an overall 5-year survival rate of less than 1% (1), the primary goals of treatment for unresectable pancreatic cancer patients are to improve overall survival and palliation. Several previous studies have reported that HIFU is useful for palliative treatment in patients with unresectable pancreatic cancer (2-4).

HIFU can have both thermal and mechanical effects on tissue. However, tissue damage through thermal injury can increase the risk of releasing autodigestive enzymes, thereby leading to pancreatitis (5). In addition, the effectiveness of partial thermal ablation of the tumor remains questionable in patients with advanced pancreas cancer. It seems more rational to find a way to use HIFU to aid the chemotherapy that is necessary for patients with pancreatic cancer.

Until now, many HIFU trials have focused on enhancing the cytotoxic effect of chemotherapeutic agents in diverse cancers (6-10). In terms of pancreatic cancers, a few studies have recently reported that the concurrent use of drugs and HIFU might decrease tumor growth in pancreatic cancer compared with the use of drugs or HIFU alone (11, 12). Ultrasound-enhanced drug delivery is known to be mainly related to sonoporation (13). Previous in vitro and in vivo studies have suggested that sonoporation with acoustic

cavitation could enhance drug delivery by making microvessels porous and inducing the extravasation of macromolecular anti-cancer agents into the tumor (7, 10, 11, 14-16).

In our institute, dozens of cases with unresectable pancreatic cancer have been treated with HIFU since 2008. During the treatments, we frequently encountered patients with metallic stents in the common bile duct (CBD) because pancreatic head cancer commonly invades the CBD. The metallic stents contained either air or fluid, as usual. Because air has high reflectivity and fluid has low reflectivity at the tissue interface on ultrasound, they are the factors most likely to affect HIFU treatment. However, to the best of our knowledge, there has been no report about the effect of metallic stents and their content on the treatment of pancreatic head cancer with HIFU.

Thus, the purpose of this study was to investigate whether a cylindrical structure containing either air or fluid and with or without metallic stent affects HIFU treatment through a gel phantom study.

MATERIALS AND METHODS

Phantom preparation

The recipe for tissue-mimicking phantom preparation was similar to that reported by Lafon et al. (17). This phantom is based on a polyacrylamide gel mixed with bovine serum albumin (BSA), a protein used as a temperature-sensitive indicator (18). The following protocol for phantom fabrication was used: Degassed, distilled water and 1 mol/L TRIS buffer at pH 8 (Biosesang, Seongnam, Bundang, Korea) were mixed to dissolve the 4.05g BSA at concentrations of 9% (by weight). A 40% w/v acrylamide solution (Biosesang, Seongnam, Bundang, Korea) with a 19:1 ratio of acrylamide: bis acrylamide in solution was added. The polymerization was initiated by the addition of a 10% (w/v) ammonium persulfate solution (APS, Biosesang, Seongnam, Bundang, Korea) and N,N,N_,N_-tetramethylethylene/ diamine (TEMED, Biosesang, Seongnam, Bundang, Korea) redox system at room temperature.

The size of the phantom was 5 cm along the x-axis, 8.5 cm along the y-axis, and 7 cm along the z-axis. A cylindrical hole 1 cm in diameter simulating a common bile duct in the pancreatic head was made in the phantom (Fig. 1). In total, 16 phantoms were prepared. The 16 phantoms consisted of 4 groups: a group of 4 phantoms with air in the holes (Group 1); a group of 4 phantoms with fluid in the holes (Group 2); a group of 4 phantoms with air-containing biliary stents (Group 3); and a group of 4 phantoms with fluid-containing biliary stents (Group 4). The biliary stent used was a Niti-S uncovered stent (TaeWoong Medical, Seoul, Korea) 10 mm in diameter and 5 cm in length.

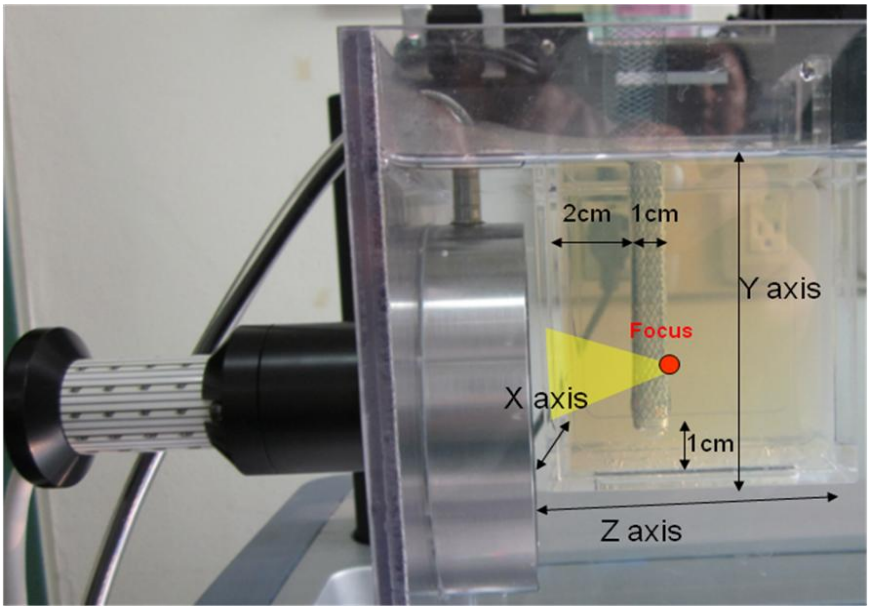

Fig. 1. Experimental design. The phantoms were 5 cm along the x-axis (width), 8.5 cm along the y-axis (height), and 7 cm along the z-axis (depth). A cylindrical hole 1 cm in diameter and 7.5 cm in height was made in the phantom. The focus of the HIFU beam was the posterior wall of the hole and 2 to 3 cm from the bottom of the phantom.

HIFU equipment and parameters

The VIFU-2000 HIFU unit (ALPINION Medical Systems, Seoul, Korea) was used to deliver HIFU. The therapeutic HIFU transducer was a fixed-focus concave transducer composed of single piezoelectric elements with an overall aperture of 82 mm and a focal depth of 44 mm. The elements of the HIFU transducer were driven in phases at a frequency of 1.1 MHz. The -6 dB focal dimensions were 9.2 mm in length and 1.3 mm in diameter (ALPINION Medical Systems, Seoul, Korea).

The HIFU beam was aimed at the posterior wall of the hole and moved automatically at -2 mm, 0 mm, +2 mm along the x-axis during insonation. Acoustic power (100 W), exposure time (36 s), duty cycle (50%) and pulse repetition frequency (40 Hz) were used, as determined in our pilot study. The posterior wall of the hole was targeted because the intrapancreatic bile duct was anatomically posterior to the pancreatic head, so that the posterior wall of the bile duct was targeted to fully cover the pancreatic head lesion.

Measuring volume of cavitation or coagulation zone

Cavitation was defined as formation of tiny bubbles in the phantom, and coagulation was defined as cloudy discoloration indicating tissue denaturation (11, 17, 19) (Fig. 2).

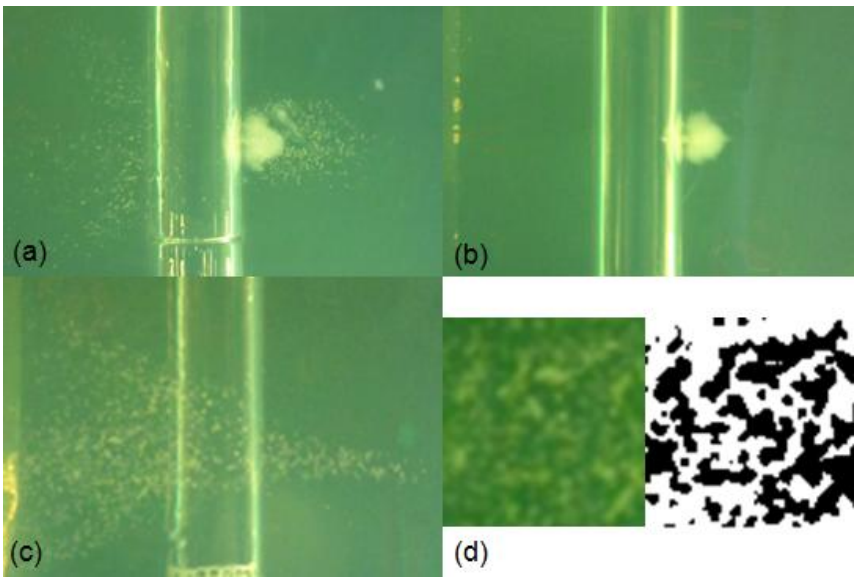

Fig. 2. (a) (b) Photographs of two phantoms from Group 2. Whereas anterior cavitation is observable in the phantom (a), no bubble is visible in the phantom (b). Both show posterior coagulation necrosis. (c) A photograph

from Group 1. The anterior cavitation in Phantom (c) is larger and denser than that in Phantom (a). (d) A 1 cm x 1 cm square in the anterior cavitation and corresponding binary image. The 'Histogram' command in ImageJ counted the number of black dots (cavitation) and white dots (remaining background). In this image, the number of black dots was 2752, and the number of white dots was 3177. Therefore, the percentage of cavitation in this phantom was 46% (2752/5929).

The cavitation extent was estimated by measuring the size along the x-, y-, and z-axis and the volume of the place where individual cavitation bubbles occurred. The coagulation extent was estimated by measuring the size on the x-, y-, and z-axis and the volume of the place where cloudy discoloration occurred. The size on the x-, y-, and z-axis of cavitation and coagulation were measured immediately after HIFU exposure, and the volume was calculated using the formula for the volume of an elliptical cone, where V is the volume, h is the height, and a and b are the semi-major and semi-minor axes of the elliptical base.

$V\ (cm3) = \pi/3 \times a\ (cm) \times b\ (cm) \times h\ (cm) = \pi/3 \times (x/2) \times (y/2) \times z$

Measuring density of cavitation by ImageJ

Under standardized conditions, images of the phantoms were taken in the yz plane with a digital camera (Canon IXUS 105, Japan). For the measurement of the cavitation density, a square 1cmf region of interest was placed, and then the density of cavitation was calculated using ImageJ

software (http://rsb.info.nih.gov/ij/) (Fig. 2). First, a binary image was created using the software's "make binary" function, in which the cavitation areas appear black, and the remaining background appears white (20). Second, an automated measurement of the cavitation ratio in a 1 cm x 1 cm square (i.e., black areas on the binary image) was performed by selecting the 'Histogram' command in ImageJ. The final binary image was carefully cross-checked with the original images of the phantoms (21).

Statistical analysis

The results are reported as the median values with minimum and maximum values. Nonparametric multiple comparisons of the cavitation volume and density between four groups were performed using the Kruskal-Wallis test and post-hoc analysis (22) and the Mann-Whitney *U* test was for 2 nonparametric independent samples with MedCalc statistical software, Version 12.2.1 (MedCalcSoftware, Mariakerke, Belgium). A P value < 0.05 was considered significant.

RESULTS

Formation of cavitation or coagulation necrosis

Tiny bubbly lesions representing acoustic cavitations were found at both the anterior and posterior sides of the HIFU focus in 8 phantoms with air (Groups 1 and 3). Cavitations were observed at the anterior side of the HIFU focus only in the half of the phantoms with fluid, 2 of the 4 phantoms (50%) in Group 2, and 2 of the 4 phantoms (50%) in Group 4. A coagulation zone formed immediately posterior to the HIFU focus in all 8 of the phantoms with fluid (Groups 2 and 4).

Volume of cavitation or coagulation necrosis

The median values with ranges for the x-axis, y-axis, z-axis and volume of the anterior and posterior cavitations and the coagulation zone in the phantoms are summarized in Table 1.

Table 1. Size and Volume of Cavitation and Coagulation Necrosis, Density of Cavitation

	Group 1	Group 2	Group 3	Group 4
Anterior cavitation				
x (cm)	4.13 (3.69-4.42)	0.88 (0-2)	3.97 (3.54-4.58)	1.04 (0-2.92)
y (cm)	2.33 (2.31-3.18)	1.21 (0-3)	2.13 (2-2.42)	1.39 (0-2.92)
z (cm)	2.84 (2.54-3.18)	1.04 (0-2.8)	2.56 (2.42-2.92)	0.81 (0-2.67)
Volume (cm^3)	7.14 (5.67-11.7)	1.15 (0-4.4)	6.03 (4.85-7.02)	1.72 (0-4.24)
Posterior cavitation				
x (cm)	0.33 (0.31-0.38)	0.76 (0.68-1.00)	0.30 (0.28-0.33)	0.36 (0.31-0.67)
y (cm)	0.35 (0.31-0.42)	0.69 (0.58-1.00)	0.33 (0.28-0.33)	0.60 (0.39-0.92)
z (cm)	1.24 (0.83-1.43)	0.91 (0.10-1.23)	1.49 (1.25-1.67)	0.91 (0.50-1.50
volume (cm^3)	0.04 (0.03-0.04)	0.12 (0.01-5.42)	0.04 (0.03-0.04)	0.05 (0.03-0.11)
Posterior coagulation necrosis				
x (cm)		0.59 (0.58-0.64)		0.64 (0.62-0.71)
y (cm)		0.58 (0.53-0.60)		0.54 (0.48-0.72)
z (cm)		0.53 (0.39-0.52)		0.54 (0.45-0.64)
volume (cm^3)		0.05 (0.04-0.05)		0.05 (0.04-0.08)
Density of anterior cavitation (yz plane, % in the area of 1x1cm)				
	0.48 (0.44-0.51)	0.005 (0-0.06)	0.45 (0.38-0.52)	0.16 (0-0.34)

Note. –values = median values with ranges, group 1= 4 phantoms with air in the holes, group 2 = 4 phantoms with fluid in the holes, group 3 = 4 phantoms with air-containing biliary stents, group 4 = 4 phantoms with fluid-containing biliary stents.

The Kruskal-Wallis test revealed a statistically significant difference in the size along the x-axis (*P* value = 0.009) and the volume (*P* value = 0.008) of anterior cavitations among the 4 groups. In the post hoc analyses, the size

along the x-axis and the volume of the anterior cavitations of Groups 1 and 3 were significantly larger than those of Groups 2 and 4 (*P* values < 0.05; Fig. 3).

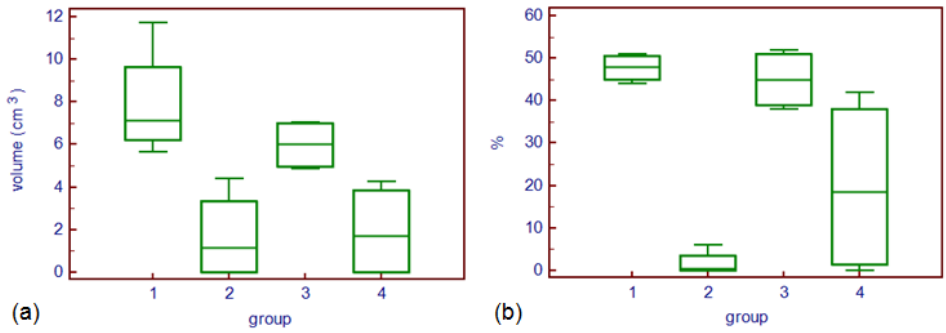

Fig. 3. Box plots of the volume (a) and density (b) of the anterior cavitations in the four groups.

The midline within the box represents the median value. Groups 1 and 3 show larger and denser cavitation compared with Groups 2 and 4.

In the posterior cavitations, although the size along the x- and y-axes differed significantly among the 4 groups (all *P* values = 0.01), the size along the z-axis and the volume were not significantly different (*P* values = 0.21 and 0.53, respectively).

Regarding the comparison between anterior and posterior cavitations, in Groups 1 and 3, the size of all axes and the volumes of the anterior cavitations were significantly larger than those of the posterior cavitations (*P* values < 0.05). However, in Groups 2 and 4, the size of all axes and the volumes of the anterior cavitations were not significantly different from those of the posterior cavitations (*P* values > 0.05).

Regarding the comparison between Groups 1 and 3 (phantoms with air in the hole) and between Groups 2 and 4 (phantoms with fluid in the hole), there was no statistically significant difference in the size of any axis and the volume of the cavitations ($P > 0.05$). Coagulation zones only appeared in Groups 2 and 4, which did not show any significant difference in the size of any axis and the volume of coagulation ($P > 0.05$).

Density of cavitation measured with ImageJ

The median values, with the ranges of the densities of the anterior cavitations on the yz plane, are summarized in Table 1. A comparison of the four groups showed that the densities of the anterior cavitations of Groups 1 and 3 differed significantly from those of Groups 2 and 4 (P value < 0.05; Fig. 3). Because of the small number of bubbles, ImageJ was not technically feasible for the posterior cavitations

DISCUSSION

Our study showed that phantoms with air-containing holes (Groups 1 and 3) had larger and denser anterior cavitations compared with phantoms with fluid-containing holes (Groups 2 and 4), regardless of the presence of stent. In addition, anterior cavitations were significantly larger than posterior cavitations in phantoms with air-containing holes, regardless of the presence of stent, whereas the sizes of anterior and posterior cavitations did not differ in phantoms with fluid-containing holes. Coagulation zones were found at the posterior side of the HIFU focus only in the phantoms with fluid-containing holes (Groups 2 and 4). Because the pancreatic head is located at the anterior aspect of the main pancreatic duct, our results suggest that air-containing CBDs may produce cavitations in a wider area of the surrounding pancreatic cancer compared with fluid-containing CBDs.

Acoustic cavitation is a mechanical phenomenon that occurs when a gas-filled bubble interacts with an ultrasound field because the rupture of cavitating bubbles (inertial cavitation) delivers high temperature and high pressure to adjacent tissue and cells (5, 23-25). In addition, this phenomenon is known to be important for reaching the temperature of *thermal fixation,* at which the cells do not undergo lysis and the tissue architecture remains relatively intact, but the cells are no longer viable, and for avoiding coagulation necrosis, which can cause pancreatitis (5). Although cavitation has been shown to be beneficial, if it occurs in the wrong region,it can cause reversible or irreversible damage to the wrong tissue (26). According to our

results, a cylindrical hole filled with air might be more useful than a cylindrical hole filled with fluid to ensure that cavitation mainly occurs at locations where should be treated with larger volume and higher density during HIFU treatment.

In the phantoms with a fluid-containing hole with or without stents (Groups 2 and 4), the volumes of the posterior cavitations were not significantly different from those of the anterior cavitations. This outcome differed from our expectation that posterior cavitations would be larger than anterior cavitations in Groups 2 and 4 because fluid has much lower reflectivity than air does. Instead, posterior coagulation necrosis was observed in Groups 2 and 4. Therefore, we presumed that the defocusing associated with high transmission in the fluid resulted in posterior coagulation instead of posterior cavitation. In addition, anterior cavitations were observed in half of the subjects in Groups 2 and 4, respectively. We also presumed that a significant change in the reflection of the HIFU beam resulting from a minimal difference in the focusing area might be related to the inconsistent formation of anterior cavitation in the phantoms with fluid. Regardless, both posterior coagulation and inconsistent anterior cavitation are undesirable for HIFU treatment of pancreas cancer.

There are several limitations to our study. First, the small number of phantoms in each group could unfavorably influence the statistical analysis in our study, even though our study exhibited relatively consistent results. Second, we used the formula for the volume of an elliptical cone. Actual cavitation or coagulation necrosis might not be precisely the shape of an

elliptical cone. However, the elliptical cone was the solid figure most like the shape of the studied necrosis, and we were able to obtain consistent results using that formula. Third, we analyzed the density of anterior cavitation on the yz plane. Although three-dimensional (3D) analysis is identical, it has many practical limitations. The limitation of the 2D analysis was the possibility of underestimation caused by the overlapping of different bubbles. However, our analysis using ImageJ digitized the 2D image and revealed significant differences between Groups 1 and 3 and Groups 2 and 4. Fourth, in our study, the HIFU beam was aimed only at the posterior wall of the hole. In clinical practice, the HIFU beam is often aimed both at the anterior and posterior wall of the hole. However, in the case of HIFU beam at the anterior wall of the CBD, the tumor encasing the CBD cannot be damaged sufficiently. Therefore, we aimed the HIFU beam at the posterior wall of the hole in this study. Lastly, human pancreatic tumors are larger and deeper than those of phantom models. Therefore, further study is needed to reoptimize the HIFU parameters.

In conclusion, phantoms with air-containing holes developed larger and denser cavitations anterior to the focus without unnecessary ablation posterior to the focus, regardless of the presence of stents. The result of this study could be used to maximize cavitation to enhance drug delivery into tumors.

REFERENCE

1. Ries L, Melbert D, Krapcho M, Stinchcomb D, Howlader N, Horner M, et al. SEER cancer statistics review, 1975-2005. Bethesda, MD: National Cancer Institute. 2008:1975-2005.

2. Wu F, Wang Z-B, Zhu H, Chen W-Z, Zou J-Z, Bai J, et al. Feasibility of US-guided High-Intensity Focused Ultrasound Treatment in Patients with Advanced Pancreatic Cancer: Initial Experience1. Radiology. 2005;236(3):1034-40.

3. Xiong LL, Hwang JH, Huang XB, Yao SS, He CJ, Ge XH, et al. Early clinical experience using high intensity focused ultrasound for palliation of inoperable pancreatic cancer. Jop. 2009;10(2):123-9.

4. Zhao H, Yang G, Wang D, Yu X, Zhang Y, Zhu J, et al. Concurrent gemcitabine and high-intensity focused ultrasound therapy in patients with locally advanced pancreatic cancer. Anti-cancer drugs. 2010;21(4):447-52.

5. Jang HJ, Lee J-Y, Lee D-H, Kim W-H, Hwang JH. Current and future clinical applications of high-intensity focused ultrasound (HIFU) for pancreatic cancer. Gut and liver. 2010;4(Suppl 1):S57-S61.

6. Paparel P, Curiel L, Chesnais S, Ecochard R, Chapelon JY, Gelet A. Synergistic inhibitory effect of high-intensity focused ultrasound combined with chemotherapy on Dunning adenocarcinoma. BJU international. 2005;95(6):881-5.

7. Iwanaga K, Tominaga K, Yamamoto K, Habu M, Maeda H, Akifusa S, et al. Local delivery system of cytotoxic agents to tumors by focused sonoporation. Cancer gene therapy. 2007;14(4):354-63.

8. Lentacker I, Geers B, Demeester J, De Smedt SC, Sanders NN. Design and evaluation of doxorubicin-containing microbubbles for ultrasound-triggered doxorubicin delivery: cytotoxicity and mechanisms involved. Molecular Therapy. 2009;18(1):101-8.

9. Daigeler A, Chromik AM, Haendschke K, Emmelmann S, Siepmann M, Hensel K, et al. Synergistic effects of sonoporation and taurolidin/TRAIL on apoptosis in human fibrosarcoma. Ultrasound in medicine & biology. 2010;36(11):1893-906.

10. Lee NG, Berry JL, Lee TC, Wang AT, Honowitz S, Murphree AL, et al. Sonoporation enhances chemotherapeutic efficacy in retinoblastoma cells in vitro. Investigative Ophthalmology & Visual Science. 2011;52(6):3868-73.

11. Lee ES, Lee JY, Kim H, Choi Y, Park J, Han JK, et al. Pulsed high-intensity focused ultrasound enhances apoptosis of pancreatic cancer xenograft with gemcitabine. Ultrasound in medicine & biology. 2013 Nov;39(11):1991-2000. PubMed PMID: 23972483.

12. Lee JY, Choi BI, Ryu JK, Kim Y-T, Hwang JH, Kim SH, et al. Concurrent chemotherapy and pulsed high-intensity focused ultrasound therapy for the treatment of unresectable pancreatic cancer: initial experiences. Korean Journal of Radiology. 2011;12(2):176-86.

13. Liang H, Tang J, Halliwell M. Sonoporation, drug delivery, and gene therapy. Proceedings of the Institution of Mechanical Engineers, Part H: Journal of Engineering in Medicine. 2010;224(2):343-61.

14. Bazan-Peregrino M, Arvanitis CD, Rifai B, Seymour LW, Coussios C-C. Ultrasound-induced cavitation enhances the delivery and therapeutic

efficacy of an oncolytic virus in an< i> in vitro</i> model. Journal of Controlled Release. 2012;157(2):235-42.

15. Hancock HA, Smith LH, Cuesta J, Durrani AK, Angstadt M, Palmeri ML, et al. Investigations into Pulsed High-Intensity Focused Ultrasound–Enhanced Delivery: Preliminary Evidence for a Novel Mechanism. Ultrasound in medicine & biology. 2009;35(10):1722-36.

16. Ohl C-D, Arora M, Ikink R, de Jong N, Versluis M, Delius M, et al. Sonoporation from jetting cavitation bubbles. Biophysical journal. 2006;91(11):4285-95.

17. Lafon C, Zderic V, Noble ML, Yuen JC, Kaczkowski PJ, Sapozhnikov OA, et al. Gel phantom for use in high-intensity focused ultrasound dosimetry. Ultrasound in medicine & biology. 2005;31(10):1383-9.

18. Bouchard LS, Bronskill MJ. Magnetic resonance imaging of thermal coagulation effects in a phantom for calibrating thermal therapy devices. Medical physics. 2000 May;27(5):1141-5. PubMed PMID: 10841421.

19. Maxwell AD, Wang TY, Yuan L, Duryea AP, Xu Z, Cain CA. A tissue phantom for visualization and measurement of ultrasound-induced cavitation damage. Ultrasound in medicine & biology. 2010 Dec;36(12):2132-43. PubMed PMID: 21030142. Pubmed Central PMCID: 2997329.

20. Foerch C, Arai K, Jin G, Park KP, Pallast S, van Leyen K, et al. Experimental model of warfarin-associated intracerebral hemorrhage. Stroke; a journal of cerebral circulation. 2008 Dec;39(12):3397-404. PubMed PMID: 18772448. Pubmed Central PMCID: 3712841.

21. Kameda M, Shingo T, Takahashi K, Muraoka K, Kurozumi K,

Yasuhara T, et al. Adult neural stem and progenitor cells modified to secrete GDNF can protect, migrate and integrate after intracerebral transplantation in rats with transient forebrain ischemia. The European journal of neuroscience. 2007 Sep;26(6):1462-78. PubMed PMID: 17880388.

22. Conover W. Practical nonparametric statistics. 1980. J Wiley&Sons.

23. Hwang JH, Tu J, Brayman AA, Matula TJ, Crum LA. Correlation between inertial cavitation dose and endothelial cell damage< i> in vivo</i>. Ultrasound in medicine & biology. 2006;32(10):1611-9.

24. Prentice P, Cuschieri A, Dholakia K, Prausnitz M, Campbell P. Membrane disruption by optically controlled microbubble cavitation. Nature Physics. 2005;1(2):107-10.

25. Kim Y-s, Rhim H, Choi MJ, Lim HK, Choi D. High-intensity focused ultrasound therapy: an overview for radiologists. Korean Journal of Radiology. 2008;9(4):291-302.

26. Thomas CR, Farny CH, Coussios CC, Roy RA, Holt RG. Dynamics and control of cavitation during high-intensity focused ultrasound application. Acoustics Research Letters Online. 2005;6:182.

국문 초록

서론: 본 연구의 목적은 겔 모형을 이용하여 고강도 집중 초음파 (HIFU) 에 의해 겔 모형 속에 생성되는 공동화가 겔 모형 속 원통형 관에 공기 또는 물을 채웠을 때, 또 원통형 관에 금속 스텐트를 설치 했을 때 공동화의 부피와 밀도가 어떤 조건에서 얼마나 영향을 받는지 조사하고자 한다.

방법: 원통형 관이 있는 열 여섯 개의 겔 모형을 네 그룹으로 나뉘었는데, 그룹 1 은 원통형 관에 공기를 채운 4 개의 모형, 그룹 2 는 원통형 관에 물을 채운 4 개의 모형, 그룹 3 는 원통형 관에 금속 스텐트를 넣고 그 속에 공기를 채운 4 개의 모형, 그룹 4 는 원통형 관에 금속 스텐트를 넣고 그 속에 물을 채운 4 개의 모형으로 이루어졌다. VIFU-2000 소형 동물용 고강도 집중 초음파 (알피니언, 서울, 대한 민국)를 100W 의 음파 출력, 36 초의 노출 시간, 50%의 동작 비율, 40Hz 의 펄스 반복 주파수로 사용하였다. 고강도 집중 초음파 빔의 초점은 모형 속 원통형 관의 후벽에 맞추었다. x 축, y 축, z 축을 기준으로 공동화 혹은 응고된 부분의 크기를 측정하였고, 이를 바탕으로 타원뿔의 부피 공식을 이용하여 부피를 계산하였다. 공동화된 부분의 밀도는 겔 모형의 yz 면에서 원통형 관의 바로 앞에 한 면이 1cm 인 정사각형을 그려 측정하였다. 통계 분석에는 Kruskal-Wallis test 와 Mann-Whitney U test 가 사용되었다.

결과: 그룹 1 과 3 에서 원통형 관 앞쪽으로 공동화된 부분의 부피가 그룹 2 와 4 의 공동화 부분의 부피보다 통계적으로 유의하게 컸다($P < 0.05$). 반면 원통형 관 뒤쪽으로 공동화된 부분의 부피는 네 그룹 간에 유의한 차이를 보이지 않았다 ($P > 0.05$). 원통형 관 앞쪽으로 공동화된 부분의 부피와 크기는 뒤쪽의 공동화된 부분보다 유의하게 컸다 ($P < 0.05$). 그룹 1 과 3 의 앞쪽 공동화된 부분의 밀도가 그룹 2 와 4 에서 측정된 밀도보다 높았다 ($P < 0.05$).

결론: 본 연구의 결과는 스텐트 유무에 관계 없이, 관에 공기를 채웠을 때 고강도 집중 초음파로 공동화 형성을 최대화할 수 있음을 보여주며, 이는 종양으로의 약물 전달을 최대화 하는데 도움을 줄 수 있다.

주요어: 고강도 집중 초음파, 공동화, 진행성 췌장암, 스텐트, 공기, 물, 겔 모형

학 번: 2012-21670